Serbian Tribology Society

SERBIATRIB '15

14th International Conference on Tribology

University of Belgrade, Faculty of Mechanical Engineering

Belgrade, Serbia, 13 – 15 May 2015

THE TRIBOLOGICAL PERFORMANCE OF HARDFACED/THERMAL SPRAYED COATINGS FOR INCREASING THE WEAR RESISTANCE OF VENTILATION MILL WORKING PARTS

Aleksandar VENCL[1,*], Boris KATAVIĆ[2], Danijela MARKOVIĆ[1], Marko RISTIC[2], Bojan GLIGORIJEVIĆ[3]

[1]University of Belgrade, Faculty of Mechanical Engineering, Belgrade, Serbia

[2]Institute Goša, Belgrade, Serbia

[3]University of Belgrade, Innovation Centre of Technology and Metallurgy in Belgrade, Belgrade, Serbia

*Corresponding author: avencl@mas.bg.ac.rs

Abstract: *During the coal pulverizing, the working parts of the ventilation mill are being worn by the sand particles. For this reason, the working parts are usually protected with materials resistant to wear (hardfaced/thermal sprayed coatings). The aim of this study was to evaluate the tribological performance of four different types of coatings as candidates for wear protection of the mill's working parts. The coatings were produced by using the filler materials with the following nominal chemical composition: NiFeBSi-WC, NiCrBSiC, FeCrCTiSi, and FeCrNiCSiBMn, and by using the plasma arc welding and flame and electric arc spraying processes. The results showed that Ni-based coatings exhibited higher wear resistance than Fe-based coatings. The highest wear resistance showed coating produced by using the NiFeBSi-WC filler material and plasma transferred arc welding deposition process. The hardness was not the only characteristic that affected the wear resistance. In this context, the wear rate of NiFeBSi-WC coating was not in correlation with its hardness, in contrast to other coatings. The different wear performance of NiFeBSi-WC coating was attributed to the different type and morphological features of the reinforcing particles (WC).*

Keywords: *coatings, hardfacing, thermal spraying, microstructure, hardness, abrasive wear, friction.*

1. INTRODUCTION

In coal-fired power plants, prior to combustion, the coal is pulverized in the ventilation mill [1]. The sand particles, which are also present, promote the intensive wear of the ventilation mill's working parts (impact blades) [2,3]. For this reason, the replacements of these parts are frequently employed, which significantly affects the productivity and energy efficiency of the entire system [1]. During the coal pulverizing, the impact plates are under the dominant influence of the abrasive and erosive wear.

Abrasive wear processes are typically classified as two-body (abrasive particles or protuberances are fixed) and three-body abrasion (abrasive particles are free to slide and/or to roll). Another system of classification divides abrasion into gouging abrasion, high-stress (or grinding) abrasion and low-stress (or scratching) abrasion [4]. The rate of material removal in two-body abrasion can be one order of magnitude higher than

that for three-body abrasion, because the loose abrasive particles abrade the solid surfaces between which they are situated only about 10 % of the time, while they spend about 90 % of the time rolling [5]. Pin abrasion testing (ASTM G 132), used in this study, simulates two-body abrasion and offers a possibility for comparison of different materials relatively easy and in short period of time, with good reproducibility.

Nowadays, in order to increase the endurance of the working parts in such aggressive environment, the advanced wear resistant coatings are applied instead of conventional steel components [6]. In a recent review of such coatings, Mendez et al. [6] have emphasized the roles of the Ni-WC and Fe-based overlays with chromium-carbides. They have also highlighted the role of chromium carbides, as the reinforcing phase, and that of the boron, in terms of structural refinement.

Compared to other carbides, the WC particles are well known to their high hardness and toughness [6]. The dissolution of these particles in Ni-based matrix is usually accompanied with the lower wear resistance [7]. For this reason, the Ni-WC overlays are usually deposited by employing the processes with high heat input (HI) control, such as plasma transferred arc (PTA) process or laser beam welding [6]. These processes enable the elimination of hotter melts and longer cooling times. In contrast, the conventional welding processes usually exhibit poor HI control and high HI. Another important consideration in Ni-WC system is the presence of chromium in amounts higher than 8 %, which can cause the poor wear properties due to a presence of re-precipitated chromium carbides with low toughness [6,7].

In this study, we have compared the tribological performances of four types of hardfaced/thermal sprayed coatings. Two Ni-based coatings were reinforced either with WC or Cr-carbide/boride particles, whereas the two Fe-based coatings were reinforced with Cr-carbides or Cr-carbides/borides. The coatings were deposited by using the plasma transferred arc (PTA), flame spray (FS) and electric arc spray (AS) deposition processes. The structural and hardness properties were also analyzed.

2. EXPERIMENTAL DETAILS

2.1 Materials

The substrate material was a hot-rolled S355J2G3 steel with dimensions of 150 × 150 × 15 mm. Filler materials were manufactured by Castolin Eutectic Ltd, Vienna. Table 1 shows their nominal chemical composition and starting form. In addition, Table 1 shows depositing methods that were employed in the case of each type of the filler material. All coatings were produced in a single pass (one layer).

Table 1. Filler materials designation, nominal chemical composition, starting form and employed depositing method

Designation	Chemical composition	Form	Depositing method[1]
PG 6503	NiFeBSi-WC	powder	PTA
B 12496	NiCrBSiC	powder	FS with fusing[2]
ARC 502	FeCrCTiSi	wire	AS
E 06361N	FeCrNiCSiBMn	powder	FS with fusing[2]

[1]PTA, FS, and AS stand for plasma transferred arc welding, flame spraying, and electric arc spraying deposition method; [2]spray and fuse process

2.2 Deposition of coatings

Table 2 shows the parameters that were employed for deposition of the filler materials, to produce the corresponding coatings.

Table 2. Hardfacing/thermal spraying parameters and the deposition rates

Filler material (coating)	Process	U [V]	I [A]	Deposition rate [g/min]
PG 6503	PTA	24	85	70
B 12496	FS	24	83	72
ARC 502	AS	30	170	–
E 06361N	FS	32	175	75

Figure 1 shows the experimental setups for PTA and FS processes. In the case of B 12496 and E 06361N coatings, prior to deposition, the substrates were preheated at 80 – 110 °C. During the deposition, the substrates reached temperature of ≈ 300 °C. The OFW was then used for subsequent fusing to establish a better metallurgical bonding within coatings and between coatings and substrates. Fusing was performed at 1020 – 1050 °C for 4 min.

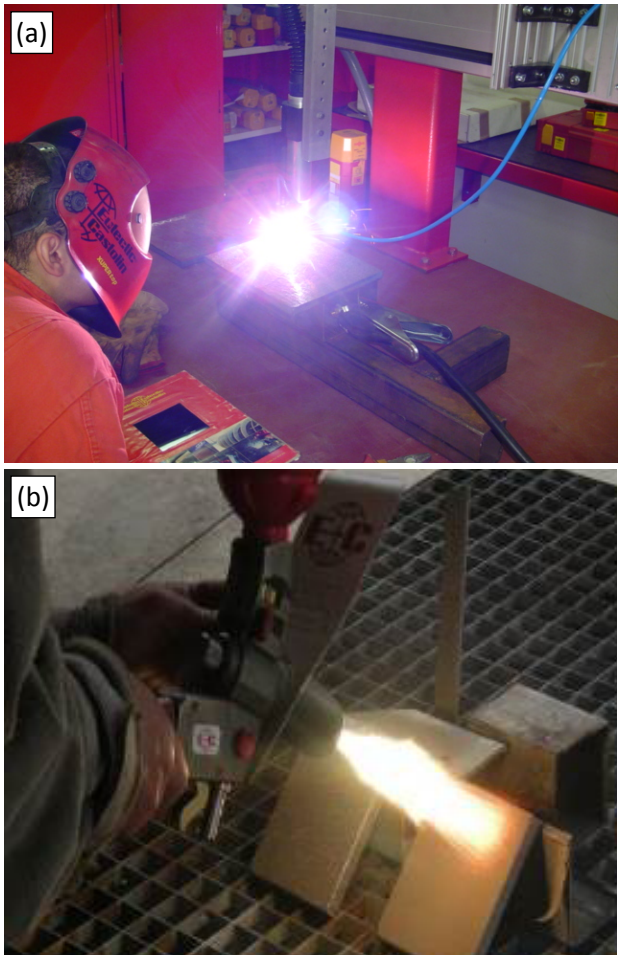

Figure 1. Experimental setup for: (a) PTA deposition and (b) FS deposition

2.3 Microstructure, density, thickness and macrohardness characterization

The samples for structure characterization were obtained by cross-sectional water jet cutting of the hardfaced/thermal sprayed coatings perpendicularly to the coating/substrate interface. The obtained cross-sections were then grinded with SiC water-proof abrasive papers down to P1200 and subsequently polished with alumina suspensions down to 1 µm. The polished surfaces were then analyzed by using the scanning electron microscope (SEM) equipped with energy dispersive system (EDS). The SEM-EDS analysis was performed at University of Belgrade, Faculty of Mining and Geology by using the JEOL JSM-6610LV SEM connected with the INCA350 energy dispersion X-ray analysis unit. The electron acceleration voltage of 20 kV and the tungsten filament were used. Before SEM-EDS analysis was performed, polished surfaces were 20 nm gold coated in a vacuum chamber by use of a sputter coater device.

Coating thicknesses for each sample were measured by using the SEM, whereas the coating densities were roughly calculated based on the percentage of identified microstructural constituents, i.e. based on the relative amount of phases present in coatings and based on the densities of pure phases.

The measurements of the near-surface hardness (HV 5) were performed on the cross-section of hardfaced/thermal sprayed samples by using the Vickers indenter.

2.4 Tribological testing

Abrasive wear tests were carried out on the pin-on-disc tribometer according to the standard test method for pin abrasion testing (ASTM G 132), in ambient air at room temperature (≈ 25 °C). The end of a pin, which was not rotating about its axis, was positioned perpendicular to the silicon carbide coated abrasive paper with grain size of 78 µm (P180 grit), which was supported by a flat horizontal rotating disc (100 mm in diameter; 100 rpm). Cylindrical pin (test sample), 5 mm in diameter and 30 mm long, was pressed by dead weights loading system over the abrasive paper producing the circular wear track. Surface roughness of pins before the tests was around Ra = 0.208 µm; Rt = 1.54 µm. A schematic diagram of pin-on-disc tribometer is presented in Figure 2.

Testing was performed under normal load of 20 N, i.e. under specific normal load of 1 MPa (taking into account the contact area of approximately 20 mm^2). Sliding distance of 30

m was constant, with an average sliding velocity of 0.2 m/s. The testing parameters were chosen, after numerous preliminary tests, to be as close as possible to the exploitation conditions and to provide a reasonable amount of wear in a steady-state wear conditions.

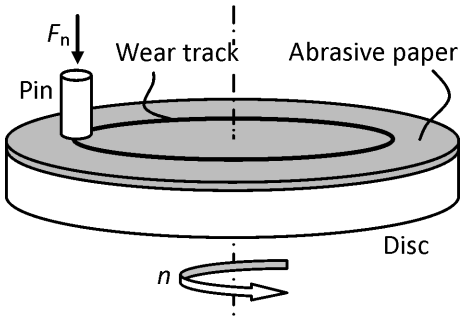

Figure 2. Schematic diagram of abrasion testing

Before and after testing, pins are cleaned with benzene. Pins were weighed with accuracy of 0.1 mg before and after each test to calculate the mass loss. Mass loss was used to calculate the wear intensity for each coating. The value of friction force was monitored during the test and through data acquisition system stored in the PC, enabling the calculation of friction coefficient. For each coating, in order to achieve a higher confidence level in evaluating test results, the three replicate tests were performed and the results were averaged.

After testing, the roughness of the test samples worn surfaces was examined with mechanical profilometer, in the direction normal to the wear tracks.

The measurements of surface microhardness (HV 0.025), before and after testing, were performed on the hardfaced/ thermal sprayed samples by using the Vickers indenter to estimate the microhardness increase during the testing.

3. RESULTS AND DISCUSSION

3.1 Microstructure, density, thickness and macrohardness characteristics

The near-surface structure of PG 6503 coating consisted of large WC grains (light phase, Fig. 3a) embedded in the Ni-based matrix (dark phase, Fig. 3a) in which Fe was dissolved in a major amount, whereas Si and B were dissolved in minor amounts. In many locations, the small, worm-like, and random-oriented WC particles were also observed. The distribution of large WC particles (120 ± 31 μm) was non-uniform in coating's thickness direction but their presence was largest in the near-surface region of PG 6503 coating. In the left-lower corner of Figure 3a, the magnified detail of the near-surface structure is shown. The arrow shows the interfacial line separating the matrix with and without worm-like WC particles. This feature was probably the consequence of deposition of welding seams one next to another.

The matrix of B 12496 coating (lightest background, Fig. 3b) was dominantly composed of Ni, while Si was dissolved as a minor element. Along the Ni grain boundaries, the network of sub-micron size particles was observed. Inside this network, light-gray and dark-gray particles co-existed. The EDS analysis of these areas (EDS 1) showed the presence of Cr, C, B and minor amounts of Fe (Fig. 4a). The light-gray and dark gray sub-micron particles were chromium-based carbides and borides, respectively. Borides of chromium possess lower density compared to the carbides of chromium and thus they appear as darker objects in backscattering electron images. Besides the boride/carbide network, there was the presence of darker few-micron size (1.6 ± 0.6 μm) particles (EDS 2), probably a mixture of chromium-based borides and carbides (Fig. 4b) that were also located between the Ni grain boundaries. Within these particles, the presence of even darker and smaller particles (probably chromium borides) was observed.

The matrix of ARC 502 coating was Fe-based with Si dissolved as a minor element (Fig. 3c). The presence of very fine sub-micron particles was uniform throughout the entire near-surface region. The EDS analysis showed that these particles were a mixture of iron- and chromium-based carbides – $(Cr,Fe)_7C_3$ (Fig. 4c). The appreciable presence of Ti was also observed. The presence of Ti suggested that the structure of these high-chromium white iron electric arc spraying layers was refined.

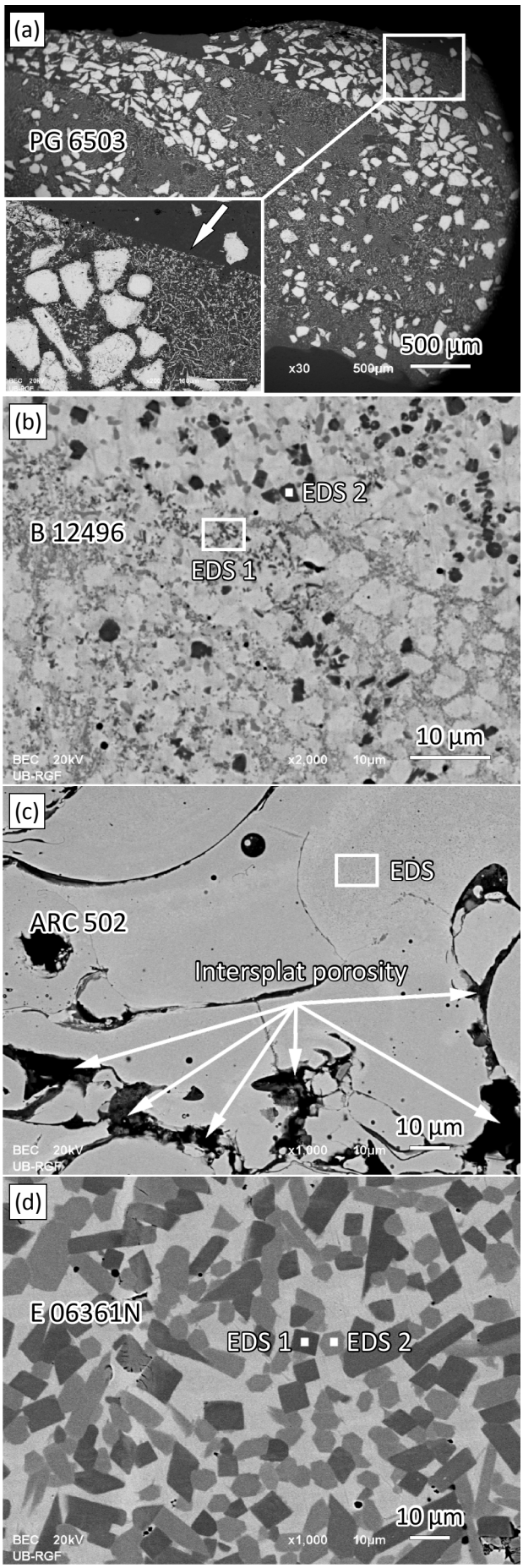

Figure 3. Microstructure properties of tested coatings

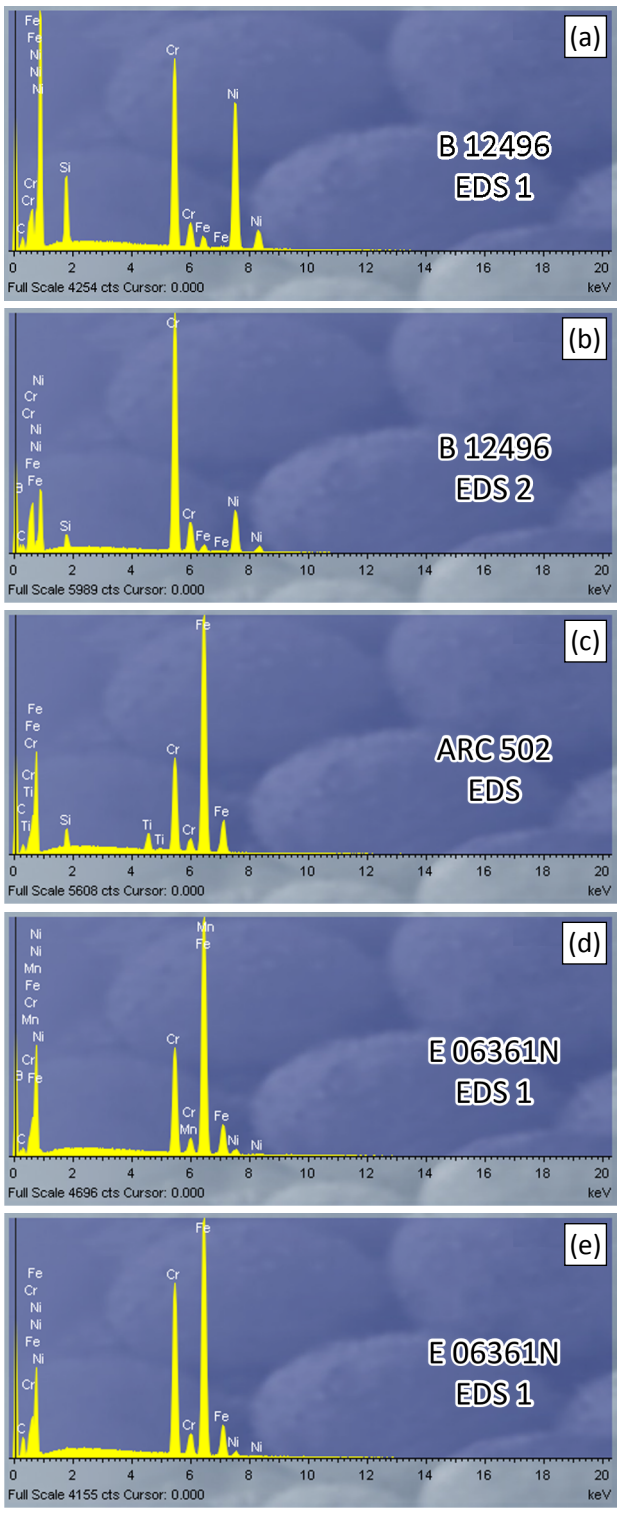

Figure 4. EDS spectra collected from cross-sections of tested coatings showed in Figure 3

The matrix of E 06361N coating was Fe-based with Si dissolved as a minor element (Fig. 3d). The reinforcing particles were chromium-based borides (darker) and carbides (lighter). The average size of these carbides was 12.0 ± 4.0 µm, in both cases. Figures 4c and 4d show the EDS spectra of boride (EDS 1) and carbide (EDS 2) reinforcing particles,

respectively. The larger intensity of Fe in comparison to EDS spectra from Figure 3b (Figs. 4a and 4b) is due to a matrix interference.

The similarities/differences between the observed structures were as follows.

Both PG 6503 and B 12496 coatings were composed of similar Ni-based matrix but different type, size and distance between the reinforcing particles. In PG 6503 coating, the large WC carbides (120 ± 31 µm) were randomly oriented and most abundant in the top surface layers of coatings (Fig. 3a). In B 12496 coating, the reinforcing particles were 75 times smaller than WC grains (Fig. 3b) and were relatively homogeneously distributed. In the near-surface region of PG 6503 coating, the WC particle-to-particle distance was between several tens to several hundreds of µm, whereas in B 12496 coating, the borides/carbides particle-to-particle distance was 20 µm at the most.

For the similar type of matrix (Ni-based), PG 6503 and B 12496 coatings possessed different hardness (Table 3). The B 12496 coating exhibited somewhat higher hardness. In general, the higher hardness of B 12496 coating was attributed to the presence of small chromium-based boride/carbide reinforcing particles and their short interparticle distance which strengthened more effectively the Ni-based matrix than large WC particles in the case of PG 6503 coating.

Table 3. Physical-mechanical characteristics of tested coatings

Coating	Density [g/cm^3]	Thickness [mm]	Hardness HV 5
PG 6503	12.9	2.65	532 – 739
B 12496	8.4	1.50	701 – 891
ARC 502	7.1	0.90	303 – 401
E 06361N	7.4	2.50	509 – 781

The ARC 502 (Fig. 3c) and E 06361N (Fig. 3d) coatings possessed the same type of Fe-based matrix. However, the relative amount of the hard reinforcing particles was obviously higher in the case of E 06361N coating. This was the possible reason why this coating exhibited higher hardness than ARC 502 coating (Table 3).

Interestingly, for the different type of reinforcing particles inside the different type of matrix and for the different type of deposition process, PG 6503 and E 06361N coatings showed the similar level of hardness and similar variation in hardness.

Figure 5 shows a typical example of hardness distribution along the thickness of tested coatings. The largest variation in hardness was observed in the case of PG 6503 and the lowest in the ARC 502 coating. The variations in hardness were attributed to the non-uniform distribution of reinforcing particles. Coating densities and thicknesses are also presented in Table 3.

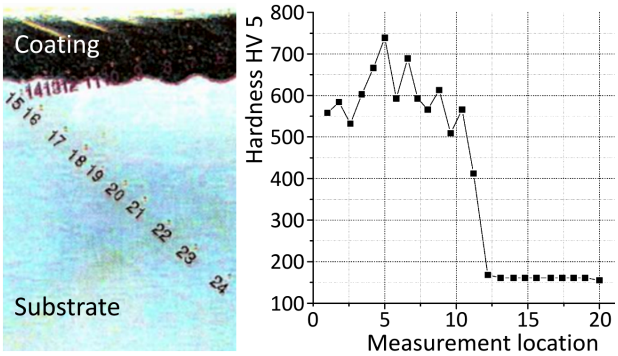

Figure 5. The hardness distribution along the thickness of PG 6503 coating (hardness measurement locations and corresponding hardness values)

3.2 Tribological properties

Tribological investigation of these coatings was just an initial one, with preliminary results and some more experiments have to be done to completely understand tribological behaviour of these coatings.

The results of the abrasion testing are presented in Figures 6 and 8. Taking into account the differences in structure homogeneity of the hardfaced/thermal sprayed coatings (Fig. 3), the repeatability of the results, in terms of standard deviations, was satisfactory. Additionally, the coefficient of variation (V_r) was calculated as standard deviation divided by the average value and then multiplied with 100 percent. The wear rate coefficients of variation (Fig. 6) were acceptable (approx. 11 %), except for coating PG 6503 (17 %). Higher coefficient of variation

for coating PG 6503 could be explained with the accuracy of weighing (0.1 mg), if it is known that the mass losses for this coating in three replicate tests were: 0.3, 0.4 and 0.3 mg. Moreover, this coating exhibited the highest level of structural heterogeneity compared to other coatings (Fig. 3). The coefficient of friction coefficients of variation (Fig. 8) are much better, i.e. within 4 %.

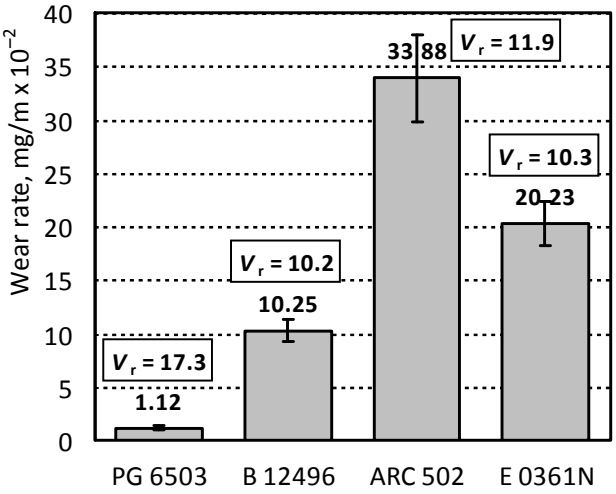

Figure 6. Wear rates of tested coatings (V_r = coefficient of variation [%])

Generally, Ni-based coatings (PG 6503 and B 12496) showed lower wear rates than Fe-based coatings (ARC 502 and E 06361 N).

The wear rates of tested coatings (Fig. 6) were in correlation with their hardness (Table 3), with the exception of coating PG 6503. The size of the reinforcing WC particles (120 ± 31 μm) in this coating was higher that the average size of the abrasive particles (78 μm), Fig. 7 (left), which was not the case in other three coatings, Fig. 7 (middle and right). In other words, and in a very simplified manner, when the size of the second phase is small relative to the abrasive groove depth, the second phase has little or no beneficial effect. In addition, the volume fraction of the secondary (reinforcing) phase in coating PG 6503 was obviously higher than in the case of other Ni-based coating (B 12496), Fig. 3. It is known that the higher volumetric fraction of the reinforcing phase implies higher abrasive wear resistance [5].

The relationship between wear rate and hardness for other three coatings (B 12496, ARC 502, and E 06361N) was disproportional, which could be explained with coatings inhomogeneous structure. For pure metal and single phase material, wear is generally inversely proportional to the hardness. However, for the multiphase alloy, the microstructure also contributes a significant effect on the wear of the material [9]. The results of other studies have also shown that abrasion wear resistance of quenched and tempered steels has much weaker dependency on the bulk hardness [10].

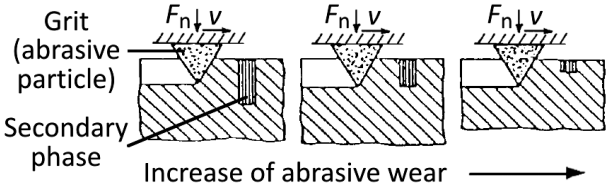

Figure 7. Effect of size of secondary (reinforcing) phase on abrasive wear (adopted from [8])

In order to compare the abrasive wear results with the results from the literature, volume wear rate (mm^3/m) and wear factor (mm^3/Nm) were also calculated (Table 4), by using the known densities (Table 3).

Table 4. Volumetric wear rates and wear factors of tested coatings

Coating	Wear rate [mm^3/m]	Wear factor [mm^3/Nm]
PG 6503	0.87 x 10^{-3}	4.34 x 10^{-5}
B 12496	1.22 x 10^{-2}	6.10 x 10^{-4}
ARC 502	4.77 x 10^{-2}	2.39 x 10^{-3}
E 06361N	2.73 x 10^{-2}	1.37 x 10^{-3}

The obtained wear factor values corresponded to the literature data for metallic materials in sliding contact (under unlubricated condition, and for abrasive wear, the interval is from 10^{-5} to 10^{-1} mm^3/Nm) [11].

Chotěborský et al. [12] have investigated high chromium Fe-Cr-C hardfacing alloys, deposited by using the gas metal arc welding (GMAW) process, on pin-on-disc tribometer, under the normal load of 23 N, and unknown type and grain size of the abrasive paper. The interval for wear rate was from 5×10^{-1} to 40×10^{-1} mg/m, which is similar to the Fe-based filler materials investigated in our study (ARC 502 and E 06361 N). One of the reasons we obtained lower values is that we did move

the pin, i.e. the pin was only at the first lap in contact with the unused abrasive paper.

On the other hand, in the case of Fe-based filler material deposited by using the open arc welding process, Kumar et al. [9] have obtained very similar wear rates (approximately 2×10^{-2} mm^3/m) compared to our study. They have used similar apparatus for the abrasive wear test and have performed the whole tests with the unused abrasive paper, but the grain size of the SiC coated abrasive paper was smaller (53 μm) than in our study (78 μm). It is known that the bigger abrasives particles produce higher wear [13], so these two effects (unused paper and smaller grain size) somehow cancel one another and the results could be comparable with the results obtained in our study.

The coefficient of friction values, shown in Figure 8, are the averaged values. For each replicate test, steady-state value for coefficient of friction was taken. In most of the tests, the steady-state was reached for a very short sliding interval (approx. 5 m). Nevertheless, for the comparisons purpose, only last 5 m of sliding was taken into account. Attained coefficient of friction values (0.3 to 0.4) were in expected range for metals in abrasive wear conditions [4]. The order of coefficient of friction values for tested coatings (Fig. 8) was the same as the order of wear values (Fig. 6), i.e. the material with the highest wear exhibited the highest coefficient of friction (when it was in contact with the abrasive paper), and vice versa.

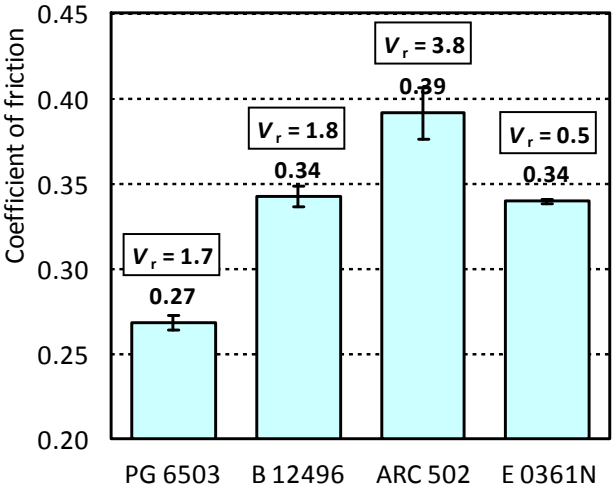

Figure 8. Coefficient of frictions of tested coatings (V_r = coefficient of variation [%])

In the case of pure abrasive wear, it was reasonable to neglect the shearing component of friction and to assume that the friction consisted only of ploughing component [14]. In such case, the coefficient of friction is proportional to the penetration depth of the abrasive particles and inversely proportional to the radius of the abrasive particles [15]. Since in our study the abrasive paper was the same for all materials (same radius of the abrasive particles), the coefficient of friction values were taken to be proportional to the yield pressure values, that is, as the first approximation, to the hardness values (Table 3).

This could not be applied for PG 6503 coating. In this type of coating, the hardness was not the only influential parameter on the penetration depth, i.e. on the coefficient of friction. This coating showed the lowest wear and the lowest surface roughness (total height of the profile, *Rt*), Fig. 9, which suggested that the penetration depth for the PG 6503 coating was the lowest.

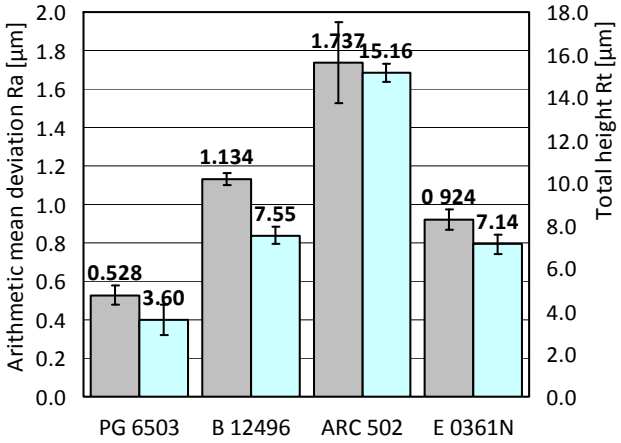

Figure 9. Surface roughness of tested coatings measured after the tests

Surface roughness of the samples, measured after the tests, is presented through the arithmetic mean deviation of the assessed profile (*Ra*) and total height of the profile (*Rt*) values (ISO 4287) in Figure 9. The order of values for tested coatings was the same as the order of coefficient of friction (Fig. 8) and wear (Fig. 6) values, i.e. the material with the highest coefficient of friction and wear shows the highest surface roughness after the test, and vice versa.

In addition to the wear and friction data, as an ancillary mechanical property, the microhardness of each of tested coatings was determined before and after the test (Fig. 10). In the Vickers microhardness test, a diamond indenter, in the form of a square-based pyramid with an angle of 136° between the opposite faces at the vertex, is used. The mean diagonal *D* and the penetration depth *H* are related as *D* = 7*H* [16]. Since the highest mean diagonal in our study was 11 µm, it means that the penetration depth of the indenter was at most 1.6 µm. This gives the relevance to the test, since the depth of the deformed layer of machined parts is usually greater than 5 µm [14].

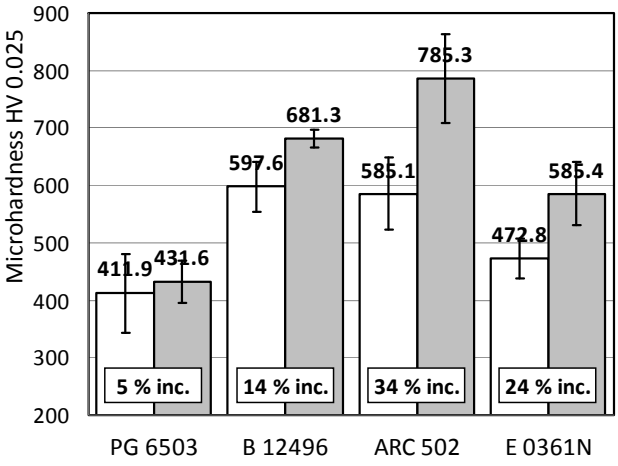

Figure 10. Microhardness of tested coatings before and after the tests (inc. = hardness increase); Microhardness of coating PG 6503 was measured only in matrix region

During abrasion, a part of the total energy is spent on cutting or ploughing, while the rest of the energy is spent on plastic deformation of the wear surface. This type of deformation causes work hardening of the subsurface and may have led to reduction in wear rate. However, after a specific sliding distance, this effect usually stabilizes and causes stable wear rate at the later stage [9]. The order of values of microhardness increase (Fig. 10) for tested coatings is the same as the order of surface roughness (Fig. 9), coefficient of friction (Fig. 8) and wear (Fig. 6) values, i.e. the material with the highest surface roughness, coefficient of friction and wear showed the highest microhardness increase during the testing, and vice versa.

Higher surface roughness and higher coefficient of friction means that there was more plastic deformation and more heat in the contact zone, thus providing more chance for case hardening.

For the investigated conditions, the lowest wear rate and coefficient of friction was obtained when Ni-based PG 6503 coating was in contact with abrasive paper. In addition, the surface roughness after the test and the increase of microhardness during the test of this sample were the lowest. Low work hardening of this coating suggested that it underwent the lowest structural changes.

Coating B 12496, with the same type of Ni-based matrix as coating PG 6503, showed higher (second lowest) increase of the wear rate and microhardness after the wear tests. In contrast to PG 6503 coating, the Ni-based matrix of coating B 12496 contained reinforcing particles (Cr-based carbides and borides, Fig. 3b), which affected the strain hardening of matrix during the wear tests by more effectively blocking the dislocation movement. On the other hand, coating E 06361N exhibited the second highest wear rate and increase of the microhardness after the wear tests. In contrast to B 12496 coating, the matrix of coating E 06361N was Fe-based with large presence (> 50 %) of Cr-based carbides and borides. The higher wear rates and higher increase of the microhardness compared to coating B 12496 were attributed to the different type of matrix and to the fact that there was a lower amount of the metal that could be deformed during the wear tests. Finally, the ARC 502 coating showed the highest wear rate and microhardness increase after the wear tests, which was mainly attributed to the presence of the sub-micron carbides distributed uniformly throughout the entire volume of coatings and the shortest distance between these reinforcing particles. Such morphological features are convenient for fast strain hardening.

The results showed that hardness was not the only characteristic that affects the wear resistance. The wear resistance of a hardfacing alloy depends on many other factors such as

the type, shape and distribution of hard phases, as well as the toughness and strain hardening behaviour of the matrix [17]. Other important factors in the abrasion resistance are the carbides orientation and the size of particles [18]. Although the PG 6503 hardfaced coating possessed the lowest hardness levels (macro and micro), it exhibited the highest resistance to abrasive wear.

4. CONCLUSIONS

In this study, the wear behaviour of four different types of hardfaced/thermal sprayed coatings was investigated (with the following types of filler materials and deposition processes): PG 6503 (NiFeBSi-WC; PTA), B 12496 (NiCrBSi; OFW), ARC 502 (FeCrCTiSi; PAW), and E 06361N (FeCrNiCSiBMn; OFW). The Ni-based coatings (PG 6503 and B 12496) showed higher wear resistance than the Fe-based coatings (ARC 502 and E 06361N).

The highest wear resistance exhibited hardfaced coating produced by using the NiFeBSi-WC filler material and PTA welding deposition process. This coating exhibited: (1) the lowest initial macrohardness, (2) the lowest wear rate and coefficient of friction during the wear tests, and (3) the lowest increase of microhardness and surface roughness after the wear tests.

The results showed that hardness was not the only characteristic that affects the wear resistance. In contrast to other coatings, the wear rate of NiFeBSi-WC coating was not in correlation with its hardness. The different wear performance of this coating was attributed to the different type and morphological features of the reinforcing particles.

ACKNOWLEDGEMENT

This work has been performed as a part of activities within the projects TR 34028 and TR 35021. These projects are supported by the Republic of Serbia, Ministry of Education, Science and Technological Development, Messer Tehnogas, and PD TE – KO Kostolac whose financial help is gratefully acknowledged.

REFERENCES

[1] M. Kozic, S. Ristic, B. Katavic, M. Puharic: Redesign of impact plates of ventilation mill based on 3D numerical simulation of multiphase flow around a grinding wheel, Fuel Processing Technology, Vol. 106, pp. 555-568, 2013.

[2] A. Alil, B. Katavić, M. Ristić, D. Jovanović, M. Prokolab, S. Budimir, M. Kočić: Structural and mechanical properties of different hard welded coatings for impact plate for ventilation mill, Welding & Material Testing, Vol. 20, No. 3, pp. 7-11, 2011.

[3] A. Vencl, B. Gligorijević, B. Katavić, B. Nedić, D. Džunić: Abrasive wear resistance of the iron- and WC-based hardfaced coatings evaluated with scratch test method, Tribology in Industry, Vol. 35, No. 2, pp. 123-127, 2013.

[4] A. Vencl, N. Manić, V. Popovic, M. Mrdak: Possibility of the abrasive wear resistance determination with scratch tester, Tribology Letters, Vol. 37, No. 3, pp. 591-604, 2010.

[5] K.-H. Zum Gahr: Wear by hard particles, Tribology International, Vol. 31, No. 10, pp. 587-596, 1998.

[6] P.F. Mendez, N. Barnes, K. Bell, S.D. Borle, S.S. Gajapathi, S.D. Guest, H. Izadi, A. Kamyabi Gol, G. Wood: Welding processes for wear resistant overlays, Journal of Manufacturing Processes, Vol. 16, No. 1, pp. 4-25, 2014.

[7] T. Liyanage, G. Fisher, A.P. Gerlich, Microstructures and abrasive wear performance of PTAW deposited Ni-WC overlays using different Ni-alloy chemistries, Wear, Vol. 274-275, pp. 345-354, 2012.

[8] K.-H. Zum Gahr: *Microstructure and Wear of Materials*, Elsevier, Amsterdam, 1987.

[9] S. Kumar, D.P. Mondal, H.K. Khaira, A.K. Jha: Improvement in high stress abrasive wear property of steel by hardfacing, Journal of Materials Engineering and Performance, Vol. 8, No. 6, pp. 711-715, 1999.

[10] G. Sundararajan: The differential effect of the hardness of metallic materials on their erosion and abrasion resistance, Wear, Vol. 162-164, Part B, pp. 773-781, 1993.

[11] K. Kato, K. Adachi: Wear mechanisms, in: B. Bhushan (Ed.): *Modern Tribology Handbook*, CRC Press, Boca Raton, Chap. 7, 2001.

[12] R. Chotěborský, P. Hrabě, M. Müller, J. Savková, M. Jirka: Abrasive wear of high chromium Fe-Cr-C hardfacing alloys, Research in Agricultural Engineering, Vol. 54, No. 4, pp. 192-198, 2008.

[13] R. Chotěborský, P. Hrabě, M. Müller, J. Savková, M. Jirka, M. Navrátilová: Effect of abrasive particle size on abrasive wear of hardfacing alloys, Research in Agricultural Engineering, Vol. 55, No. 3, pp. 101-113, 2009.
[14] A. Rac: *Basics of Tribology*, Faculty of Mechanical Engineering, University of Belgrade, Belgrade, 1991 [in Serbian].
[15] A. van Beek: *Advanced Engineering Design*, TU Delft, Delft, 2009.
[16] M.M. Yovanovich: Micro and macro hardness measurements, correlations, and contact models, in: *Proceedings of the 44th AIAA Aerospace Sciences Meeting and Exhibit*, 09-12.01.2006, Reno, USA, Paper AIAA 2006-979.
[17] J.R. Davis: Hardfacing, weld cladding, and dissimilar metal joining, in: *ASM Handbook Volume 6, Welding, Brazing, and Soldering*, ASM International, Metals Park, pp. 789-829, 1993.
[18] Ö.N. Doğan, J.A. Hawk: Effect of carbide orientation on abrasion of high Cr white cast iron, Wear, Vol. 189, No. 1-2, pp. 136-142, 1995.